Int. J. Heat Mass Transfer. Vol. 25, No. 6, pp. 781-790, 1982
Printed in Great Britain

0017-9310/82/060781-10 $03.00/0

THERMAL MODELING OF STEAM GENERATOR TUBING UNDER CHF-INDUCED TEMPERATURE OSCILLATIONS

T. T. KAO, S. M. CHO and D. H. PAI
Foster Wheeler Energy Applications, Inc., Livingston, NJ 07039, U.S.A.

(*Received* 19 *November* 1981)

Abstract—Analytical models are presented for the determination of thermal field in the heat transfer tubing under critical heat flux (CHF)-induced thermal oscillations in a sodium-heated steam generator. The oscillatory nature of the water/steam convective boundary conditions in the post-CHF transition boiling is simulated by postulating a number of rivulet-type wet regions that are swirled around the tube circumference. The rate at which the rivulets are swirled or rotated is determined by the indications of recent test data at Argonne National Laboratory. The same test data are also used as the criteria on model development. The results of 1-, 2- and 3-dim. models indicate that the 2-dim. (radial–circumferential) model with three or four rivulets and a 26.7% total circumferential wetness may be adequate for the thermal analysis of heat transfer tubing under oscillatory transition boiling.

NOMENCLATURE

A,	area;
c,	tube material specific heat;
h_f,	film boiling heat transfer coefficient;
h_i,	heat transfer coefficient at tube inner surface;
h_n,	nucleate boiling heat transfer coefficient;
h_o,	heat transfer coefficient at tube outer surface;
k,	tube thermal conductivity;
L,	tube length;
l,	modeled tube length;
n,	time step index;
N_i, N_j, N_k,	nodal point designations in ith, jth, and kth directions, respectively;
P,	pressure;
q,	heat flux;
R_i,	inner tube radius;
R_m,	interior radial position where the temperature is specified;
R_o,	outer tube radius;
r,	radial coordinate;
S,	surface area of control volume V;
T,	temperature;
T_m,	temperature at R_m;
T_s,	water/steam temperature;
T_∞,	fluid temperature outside heat transfer tube;
t,	time;
V,	volume;
z,	axial coordinate.

Greek symbols

β,	weighting function;
Δr,	incremental radial length;
ΔT_i,	temperature fluctuation amplitude at tube inner surface;
ΔT_o,	temperature fluctuation amplitude at tube outer surface;
ΔT_{T-C},	temperature fluctuation amplitude at thermocouple location;
$\Delta(\Delta T)$,	amplitude of through-the-wall temperature difference fluctuation;
Δt,	time step;
ΔV,	incremental control volume;
Δz,	incremental axial length;
$\Delta\theta$,	incremental circumferential angle;
θ,	angular coordinate;
ρ,	tube material density;
τ,	revolving rivulet period or period of temperature fluctuation;
ω_o,	base frequency.

Subscripts

CHF,	critical heat flux;
DO,	dryout;
ID,	inner diameter;
i,	ith node in radial direction;
j,	jth node in angular direction;
k,	kth node in axial direction;
o,	tube outer surface;
OD,	outer diameter;
s,	water/steam condition;
∞,	condition outside heat transfer tube.

INTRODUCTION

THE CONDITIONS of critical heat flux (CHF), or departure from nucleate boiling (DNB), occasionally exist in power plant steam generators. The flow pattern inside an evaporator tube prior to the onset of CHF/dryout is usually of annular flow type, where the liquid phase is continuous in an annulus along the tube wall and the vapor phase is continuous in the core. Discontinuous liquid phase is present in the core as droplets, while

discontinuous vapor phase appears as bubbles in the liquid annulus due to the nucleate boiling mechanism (see Fig. 1). The liquid film next to the wall gets thinner as it evaporates, eventually breaking off the wall and thus resulting in dry patches until the entire flow becomes a mist or dispersed flow in which the vapor phase is continuous and the liquid is dispersed in the vapor as droplets. In the dryout region, the wall is covered by the vapor phase and the heat transfer mechanism is that of film boiling. The heat transfer coefficient of film boiling is considerably lower than that of nucleate boiling. The difference in the heat transfer coefficient between nucleate and film boiling, and the random nature of the dryout process will produce oscillations in the tube wall temperatures, and thus thermally-induced stresses, in the evaporator tubing under transition boiling.

The CHF-induced thermal oscillations in sodium-heated steam generators have been reported in the open literature in connection with the Liquid Metal Fast Breeder Reactor (LMFBR) programs. The most recent observation was made at Argonne National Laboratory Steam Generator Test Facility (ANL-SGTF) where a single evaporator tube was tested under simulated plant operating conditions [1]. There have also been reported several analytical attempts to predict the magnitudes of CHF-induced thermal stresses, however these are limited to 1- and 2-dim. symmetric models [2, 3, 4].

The accuracy and reliability of the thermal stress prediction depends, of course, upon how the oscillatory dryout phenomenon is modeled. This paper deals with the thermal aspect of the analytical models that have been considered. One-, two- and three-dimensional thermal models are constructed. The region encompassing transition boiling is divided into a number of thermal nodes. Transient energy conservation equations are written for all nodes, and the resulting simultaneous equations, with appropriate boundary conditions, are solved numerically using a semi-implicit finite difference method.

In the 1-dim. model, a numerical inverse heat conduction method is used based on the time history of the temperature oscillations as measured experimentally by the thermocouple imbedded in a heat transfer tube which was tested at ANL-SGTF. In the 2- and 3-dim. models, the oscillatory nature of the water/steam side boundary conditions in the transition boiling region is simulated by postulating a number of rivulet-type wet regions that are swirled around the tube circumference. The rate at which the rivulets are swirled or rotated is determined by the indications of ANL-SGTF DNB tests. Comparisons between various models are made in order to establish the most suitable model and thus to provide a guideline for future design analysis.

ANL-SGTF TEST RESULTS AND PREVIOUS ANALYTICAL MODELS

Thermal oscillations induced in a sodium-heated steam generator tube wall as a consequence of unstable transition boiling have been experimentally measured at Argonne National Laboratory (ANL) Steam Generator Test Facility (SGTF). The test tube was constructed of 2¼ Cr–1 Mo steel and has dimensions of 15.875 mm o.d., 2.896 mm wall thickness [2]. A thermocouple was imbedded in the tube wall at 1.753 mm from the inside surface at an axial location of 12.2 m (40 ft) from the water inlet. Water flow was directed upward inside the tube and the heating sodium flowed downward in the annulus formed between the heat transfer tube and the shell.

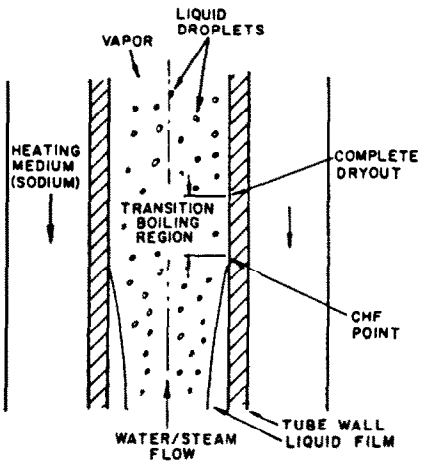

FIG. 1. Transition boiling region in steam generator tubing.

A series of tests had been conducted [1]. In Test No. R-78 which resulted in the most severe oscillations in the tube wall temperature, the water pressure, flow and inlet temperature as well as sodium flow rate were held constant while the sodium inlet temperature was adjusted in such a way that the transition boiling region would occur at the axial location of the internal tube wall thermocouple. The system controllers reduced fluctuations in the test parameters to such an extent that the internal thermocouple remained within the transition boiling region for a period of 100 min. The data shown in Fig. 2 is representative of many data scans recorded during this test. As indicated in the figure, a mean and a maximum temperature oscillation range of 12.8°C (23°F) and 17.8°C (32°F), respectively, are found.

The results of a power spectral density analysis performed on the representative data of Test No. R-78 indicate that the significant oscillations are contained in the frequencies up to 2 Hz with the decreasing magnitude above 0.8 Hz. Oscillations below 0.2 Hz are believed to be system-induced and those above 0.25 Hz are characteristic of transition boiling.

These ANL-SGTF experimental data are used as a base for the analytical thermal models.

Several 1- and 2-dim. dryout thermal models have been proposed previously. Earlier 1- and 2-dim. models are based on the wave-form models [2, 3] in which it is assumed that the temperature conditions are

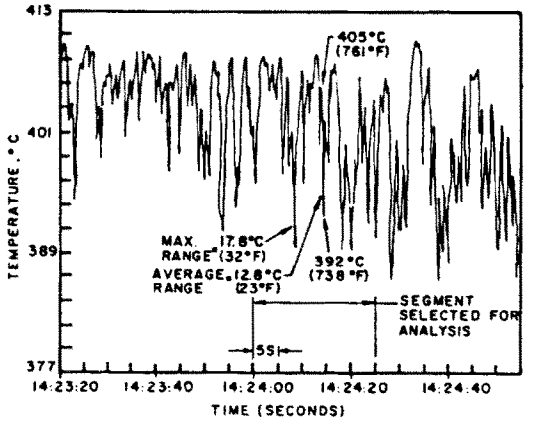

FIG. 2. Measured CHF temperature oscillations at ANL-SGTF [1].

uniform around the tube wall circumference, and the steam side heat transfer coefficient distribution takes various wave forms such as square wave, sinusoidal, trapezoid etc., along the tube length with the heat transfer mechanism varying between nucleate and film boiling. This type of model implies that the thermal oscillation is induced by the heat transfer coefficient moving back and forth along the tube. However, the spectral density analysis of ANL-SGTF measurements indicate such movement may be induced by the system parameter variations and is of low frequency nature (0.01 Hz). The CHF oscillations are observed to have a higher frequency of about 0.3 Hz.

A 1-dim. model recently proposed by France *et al.* [1] required no assumptions concerning the detail of the transition boiling phenomenon. The authors take advantage of the oscillating nature of the measured temperature of the thermocouple embedded in the tube wall of the evaporator tube. The radial temperature distribution at the axial location of the thermocouple was obtained by representing the measured temperature oscillations as a Fourier series and superimposing steady periodic heat transfer solutions for each term and frequency. The general solution was then obtained in the region between the outer tube surface and the thermocouple location, and, being steady-periodic in nature, it was readily extrapolated to the tube inside diameter. The main drawback of this model is the 1-dim. assumption. Like previous models, circumferential and axial temperature variations which are known to exist have been ignored. The thermal stress level, which is a direct function of the temperature distribution in the tube at any point in time, will be affected accordingly. Also the Fourier series representation of the measured thermocouple data is necessary to obtain the solution.

Also recently, a 2-dim. (r θ) instantaneous rivulet model has been proposed by Chu *et al.* [4] for the CHF thermal oscillation analysis. This rivulet model is based on the interpretation of the experimental results on a study of critical heat flux and flow pattern of high pressure boiling water in forced convection conducted by Tippets [5, 6]. In the model, the thermal oscillation is assumed to be produced by a number of equally spaced wet rivulets around the tube circumference. Each rivulet is assumed to remain at a given location for half of the temperature cycle and a dry region at the same location for the other half of the cycle. The appearance and disappearance of rivulets is assumed instantaneous. The birth of a new rivulet is assumed to occur at the same position as the previous rivulet. This means that part of the wall circumference is subject to alternating wet and dry regions while the other part remains dry at all times. This assumption appears to be in contradiction with the oscillatory nature of transition boiling which takes place around the entire tube circumference with equal probability. Both the number of rivulets and the percentage of wall circumference wetted by the rivulets were chosen in such a way that the upper and lower temperature fluctuation levels at the location corresponding to the imbedded wall thermocouple be matched with the experimental measurements of the ANL-SGTF test data (R-78). These investigators found that 3.7 rivulet and 21% wetness is required to produce a maximum temperature fluctuation between 407.8 C (766 F) and 389.4 C (733 F) with a period of 3 s. An integral rivulet approach was used by these authors to gain insight regarding the relative influence of the 3 and 4 rivulet cases on the stress level.

PRESENT ANALYTICAL MODELS

Two analytical models are presented in this paper. In the 1-dim. model, an inverse heat conduction method is employed. In the multi-dimensional models, the concept of revolving rivulets is introduced. These models are discussed below.

One-dimensional model analysis

France *et al.* [1] used a Fourier series to represent CHF-induced temperature oscillations obtained by the thermocouple imbedded inside the heat transfer tube that was tested at the ANL-SGTF. For Test No. R-78 (Fig. 2), this representation was accomplished by 64 sinusoidal terms:

$$1.8\,T + 32 = C_0 + \sum_{m=1}^{64} [C_m \cos(2\pi m\omega_0 t) + D_m \sin(2\pi m\omega_0 t)] \quad (1)$$

where T is the temperature in °C, ω_0 is the base frequency (0.03906 Hz), and the Fourier coefficients, C_m and D_m, can be found in [1].

In order that the measured thermocouple temperature history can be used directly to determine the tube temperature distribution, an inversed heat conduction solution technique must be used. Various approaches to this heat transfer problem have been reported in the literature. In the following a finite difference approach similar to that presented by [7] is adopted. In [7], an explicit method is used for the finite difference solution of the transient heat conduction equation in the

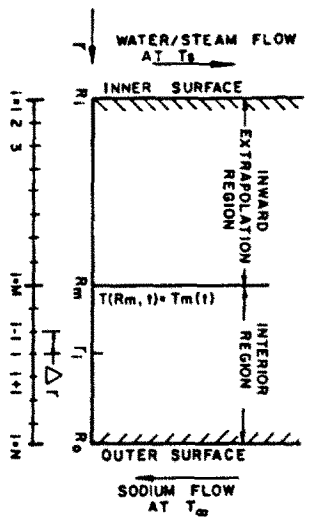

FIG. 3. One-dimensional thermal model and computational mesh for inverse heat conduction problem.

interior region bounded by two well defined boundary conditions. A non-iterative implicit method is used for the finite difference extrapolation of the interior solution to obtain the surface conditions. In the present analysis, a Crank-Nicholson type of semi-implicit finite difference algorithm is utilized throughout the wall to ensure numerical stability and higher order accuracy in solution.

Consider a 1-dim. (radial) transient heat conduction in a tube wall with the temperature history given at an interior location as may be the case with a thermocouple imbedded in the wall (Fig. 3). It is assumed that the external boundary conditions such as the (sodium) temperature and the (sodium) heat transfer coefficient are known. The problem is to determine the temperature field $T(r, t)$ between $r = R_i$ and $r = R_o$. The energy equation is given by

$$\rho c \frac{\partial T}{\partial t} = -\nabla \cdot \mathbf{q} = \frac{1}{r}\frac{\partial}{\partial r}\left(kr\frac{\partial T}{\partial r}\right). \tag{2}$$

The boundary conditions are given by

$$T(R_m, t) = T_m(t),$$
$$-k\frac{\partial T}{\partial r}\bigg|_{r=R_o} = h_o[T(R_o, t) - T_s]. \tag{3}$$

Using a semi-implicit finite differencing algorithm, one may write equation (2) in the following integral form:

$$\int_{\Delta V} \rho c \frac{\partial T}{\partial t}\,dV = \beta\left[-\int_S \mathbf{q}\cdot d\mathbf{s}\right]^{n+1} + (1-\beta)\left[-\int_S \mathbf{q}\cdot d\mathbf{s}\right]^{n} \tag{4}$$

where the superscript indicates the time step level at which the finite differencing in the space variable is being carried out, and β is a weighting function ($0 \le \beta \le 1$); $\beta = \frac{1}{2}$ for semi-implicit algorithm.

The left-hand side of the equation can be discretized at $r = r_i$ to give

$$\int_{\Delta V} \rho c \frac{\partial T}{\partial t}\,dV = (\rho c r)_i \frac{2\pi\Delta r}{\Delta t}(T_i^{n+1} - T_i^n). \tag{5}$$

Each of the square bracket terms in equation (4) can be finite differenced in the space variable

$$\left[-\int_S \mathbf{q}\cdot d\mathbf{S}\right] = 2\pi\left(r_i + \frac{\Delta r}{2}\right)\frac{k_{i+1/2}}{\Delta r}(T_{i+1} - T_i) + 2\pi\left(r_i - \frac{\Delta r}{2}\right)\frac{k_{i-1/2}}{\Delta r}(T_{i-1} - T_i). \tag{6}$$

Upon substituting equations (5) and (6) into equation (4) and, after rearrangement, the following equation is obtained:

$$A_i T_{i+1}^{n+1} + B_i T_i^{n+1} + C_i T_{i-1}^{n+1} = D_i \tag{7}$$

where

$$A_i = -\beta\left(r_i + \frac{\Delta r}{2}\right)k_{i+1/2},$$

$$B_i = (\rho c r)_i \frac{(\Delta r)^2}{\Delta t} - (A_i + C_i),$$

$$C_i = -\beta\left(r_i - \frac{\Delta r}{2}\right)k_{i-1/2},$$

$$D_i = (1-\beta)\left[\left(r_i + \frac{\Delta r}{2}\right)k_{i+1/2}(T_{i+1} - T_i) + \left(r_i - \frac{\Delta r}{2}\right)k_{i-1/2}\left(T_{i-1} - T_i\right)\right]^n + (\rho c r)_i \frac{(\Delta r)^2}{\Delta t} T_i^n.$$

As is well known, convective boundary conditions require more severe stability criteria. Thus, in order to ensure numerical stability at all times a fully implicit algorithm is used at the convective boundary. The resulting difference equation at $i = N$ (external boundary) is given by

$$A_N T_{N-1}^{n+1} + B_N T_N^{n+1} + C_N T_\infty^{n+1} = D_N \tag{8}$$

where

$$A_N = -2\left(R_o - \frac{\Delta r}{2}\right)k_{N-1/2}/\Delta r,$$

$$C_N = -2h_o R_o,$$

$$B_N = \frac{\rho c \Delta r}{\Delta t}\left(R_o - \frac{\Delta r}{4}\right) - (A_N + C_N),$$

$$D_N = \frac{\rho c \Delta r}{\Delta t}\left(R_o - \frac{\Delta r}{4}\right)T_N^n.$$

With the temperature history at the thermocouple location ($r = R_m, i = M$) given, the temperature field between $r = R_m$ and $r = R_o$ can be solved using equations (7) and (8) by the modified Gaussian

Table 1. Thermal model boundary conditions for test R-78 [2]

Evaporator tube	
Material	$2\frac{1}{4}$ Cr–1 Mo steel
i.d.	10.0838 mm (0.397 in)
o.d.	15.875 mm (0.625 in)
Thermocouple location	1.7526 mm (0.069 in) from i.d. surface
Tube wall thermal conductivity (w cm-°C)	$0.4168 - 1.616 \times 10^{-4} \times T(°C)$
Thermal conditions	
P_{ID}	11.376 MPa (1650 Psia)
P_{OD}	0.69 Mpa (100 Psia)
T_s	431°C (807.8°F)
T_s	321°C (saturated condition)
h_o	28.7 kw/m²-°C (5000 Btu/h-ft²-°F)
Additional conditions for multi-dimensional model runs	
h_n	80 Kw/m²-°C (14,000 Btu/h-ft²-°F)
h_f	4.77 Kw/m²-°C (840 Btu/h-ft²-°F)
τ	3 s
Axial length modeled	66 mm (2.6 in)

elimination procedure for tridiagonal matrix [8] to obtain $T_i (i = M \text{ to } N)$.

The numerical solution in the inverse heat conduction region bounded by the inner tube surface ($r = R_i, i = 1$) and the thermocouple ($r = R_m, i = M$) is obtained by finite difference extrapolation using equation (7), starting from $i = M$ and marching inward to $i = 2$:

$$C_i T_{i-1}^{n+1} = D_i - B_i T_i^{n+1} - A_i T_i^{n+1}; \quad i = M \text{ to } 2. \quad (9)$$

The above finite difference algorithm for inverse heat conduction solution is used to obtain the 1-dim. temperature distribution based on the thermocouple temperature oscillations as represented by a 64-term Fourier series of equation (1). Other pertinent information used in the present analysis are given in Table 1. The solution starts out with an initially assumed temperature distribution and an integration in time is performed until the solution reaches a steady-periodic condition.

The solution obtained by the present inverse heat conduction method for the evaporator tube inner wall ($i = R_i$) is shown in Fig. 4. A comparison with the solution by [1] indicates excellent agreement in terms of general shape and magnitude of oscillations. It is evident from the figure that thermal stresses are concentrated at the inner tube wall.

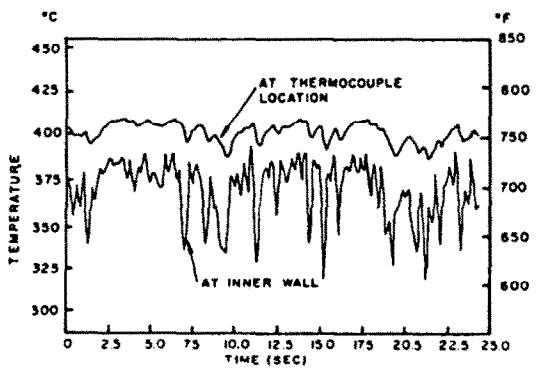

Fig. 4. Temperature oscillations at thermocouple and inner wall locations.

It is noted that the present numerical inverse heat conduction solution does not require that the thermocouple temperature fluctuations be representable in the Fourier series. It can take any form of the boundary conditions. However, this type of analysis method (this paper as well as [1]) cannot be considered as a suitable design tool because it requires measured temperature oscillations somewhere in the tube.

Multi-dimensional revolving rivulet models

In the 2-dim. (r, θ, t) rivulet model adopted in [4], the rivulets were assumed to appear and disappear instantaneously at fixed locations of the tube inner wall circumference. In the present multi-dimensional models, the rivulets are assumed to be continuously revolving around the tube circumference, in order to reduce the conservatism of the instantaneous rivulet model as well as to remove the unrealistic assumption that only part of the circumference is subjected to alternating wet and dry conditions.

A 3-dim. (r, θ, z, t) model is constructed for a section of steam generator tubing which includes the transition boiling region. The model spans radially from water/steam through tube wall to heating sodium, circumferentially around the entire circumference of the tube, and axially between fully developed nucleate and film boiling regions. The oscillating nature of water/steam side transition boiling is simulated by postulating that a number of linearly varying rivulet-type wet spots (or regions), which extend from the fully wetted CHF point to the completely dried out Leidenfrost point, swirl around the tube circumference. It should be understood, however, that the swirling of rivulets may not be actual physical occurrence, but it leads to a mathematical representation that is appropriate to seemingly random but statistically orderly (and thus capable of being modeled) transition boiling. The above model will result in axially and circumferentially alternating nucleate and film boiling heat transfer coefficients imposed on the water/steam side of the tube with the residence time of each boiling regime varying linearly along the axial direction. The number of rivulets and the frequency of alternation (0.33 Hz) are guided by the indications of the ANL-SGTF tests.

A 2-dim. (r, θ, t) rivulet model is also developed. In addition to the number of revolving rivulets, the circumferential wetness parameter is needed to match the thermal results to the ANL-SGTF test data.

Presented in the following is the necessary computational algorithm for the solution of a multi-dimensional heat conduction equation with convective boundary conditions on both inner and outer tube surfaces.

Considering a control volume ΔV, as shown in Fig.

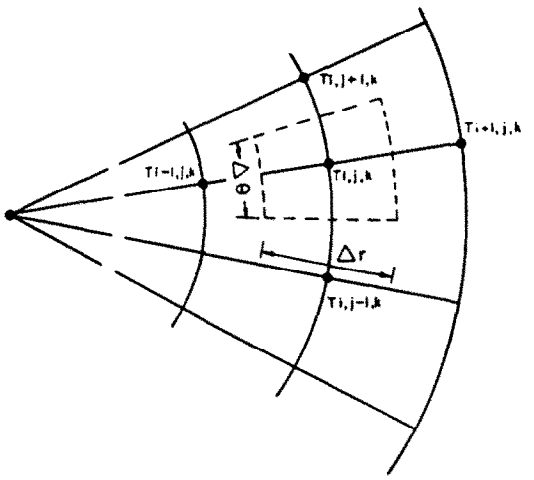

FIG. 5. Finite difference computational mesh for multi-dimensional thermal model (z dimension not shown).

5, one may write the energy equation in the same form as equation (4).

When this equation is applied to node (i, j, k), one gets

$$\frac{C}{\Delta t}(T^{n+1}_{i,j,k} - T^{n}_{i,j,k}) = \beta F^{n+1}_{i,j,k} + (1-\beta)F^{n}_{i,j,k} \tag{10}$$

where

$$\begin{aligned} F_{i,j,k} = {} & [G_F(T_{i+1,j,k} - T_{i,j,k}) + G_B(T_{i-1,j,k} - T_{i,j,k}) \\ & + G_L(T_{i,j-1,k} - T_{i,j,k}) + G_R(T_{i,j+1,k} - T_{i,j,k}) \\ & + G_U(T_{i,j,k+1} - T_{i,j,k}) + G_D(T_{i,j,k-1} - T_{i,j,k})], \\ G_F = {} & k_{i+1/2,j,k} A_{F_i}/\Delta r, \\ G_B = {} & k_{i-1/2,j,k} A_{B_i}/\Delta r, \\ G_L = {} & k_{i,j-1/2,k} A_S/(r_i \Delta\theta), \\ G_R = {} & k_{i,j+1/2,k} A_S/(r_i \Delta\theta), \\ G_U = {} & k_{i,j,k+1/2} A_T/\Delta z, \\ G_D = {} & k_{i,j,k-1/2} A_T/\Delta z, \\ A_{F_i} = {} & (r_i + \Delta r/2)\Delta\theta\Delta z, \\ A_{B_i} = {} & (r_i - \Delta r/2)\Delta\theta\Delta z, \\ A_S = {} & \Delta r\,\Delta z, \\ A_{T_i} = {} & r_i \Delta\theta \Delta r, \\ C = {} & A_{T_i}\Delta z \rho c. \end{aligned}$$

This can be further simplified to yield the following set of algebraic equations:

$$\begin{aligned} & \left[\frac{C}{\Delta t} + \beta(G_F + G_B + G_L + G_R + G_U + G_D)\right] T^{n+1}_{i,j,k} \\ & = \beta(G_F T_{i+1,j,k} + G_B T_{i-1,j,k} + G_L T_{i,j-1,k} \\ & + G_R T_{i,j+1,k} + G_U T_{i,j,k+1} + G_D T_{i,j,k-1})^{n+1} \\ & + (1-\beta)F^{n}_{i,j,k} + \frac{C}{\Delta t} T^{n}_{i,j,k} \end{aligned} \tag{11}$$

where

$$i = 2 \text{ to } N_i - 1,\ j = 1 \text{ to } N_j - 1,\ k = 2 \text{ to } N_k - 1.$$

The boundary conditions to the above set of finite differencing equations are

$$-k\left.\frac{\partial T}{\partial r}\right|_{r=R_i} = h_i(T_s - T), \tag{12}$$

$$-k\left.\frac{\partial T}{\partial r}\right|_{r=R_o} = h_o(T - T_\infty), \tag{13}$$

$$\left.\frac{\partial T}{\partial z}\right|_{z=0} = \left.\frac{\partial T}{\partial z}\right|_{z=l} = 0. \tag{14}$$

Note that the insulation boundary conditions are applied at axial locations sufficiently far away from the transition zone.

A fully implicit scheme is used in the treatment of convective boundary conditions to avoid numerical instability at the boundary nodes. Applying the boundary conditions at the inner surface nodes yields

$$\begin{aligned} \frac{\bar{C}}{\Delta t}(T^{n+1}_{1,j,k} - T^{n}_{1,j,k}) = {} & [\bar{G}_F(T_{2,j,k} - T_{1,j,k}) \\ & + \bar{G}_B(T_S - T_{1,j,k}) + \bar{G}_L(T_{1,j-1,k} - T_{1,j,k}) \\ & + \bar{G}_R(T_{1,j+1,k} - T_{1,j,k}) + \bar{G}_U(T_{1,j,k+1} - T_{1,j,k}) \\ & + \bar{G}_D(T_{1,j,k-1} - T_{1,j,k})]^{n+1} \end{aligned} \tag{15}$$

where

$$\begin{aligned} \bar{G}_F = {} & k_{3/2,j,k}\bar{A}_F/\Delta r, \\ \bar{G}_B = {} & h_i \bar{A}_B, \\ \bar{G}_L = {} & k_{1,j-1/2,k}\bar{A}_S/(R_i\Delta\theta), \\ \bar{G}_R = {} & k_{1,j+1/2,k}\bar{A}_S/(R_i\Delta\theta), \\ \bar{G}_U = {} & k_{1,j,k+1/2}\bar{A}_T/\Delta z, \\ \bar{G}_D = {} & k_{1,j,k-1/2}\bar{A}_T/\Delta z, \\ \bar{A}_F = {} & \left(R_i + \frac{\Delta r}{2}\right)\Delta\theta\Delta z, \\ \bar{A}_B = {} & R_i\Delta\theta\Delta z, \\ \bar{A}_S = {} & \Delta r\Delta z/2, \\ \bar{A}_T = {} & \left(R_i + \frac{\Delta r}{4}\right)\frac{\Delta\theta\Delta r}{2}, \\ \bar{C} = {} & \rho c \bar{A}_T \Delta z. \end{aligned}$$

This equation can be rewritten as:

$$\begin{aligned} & \left(\frac{\bar{C}}{\Delta t} + \bar{G}_F + \bar{G}_B + \bar{G}_L + \bar{G}_R + \bar{G}_U + \bar{G}_D\right) T^{n+1}_{1,j,k} \\ & = (\bar{G}_F T_{2,j,k} + \bar{G}_B T_S + \bar{G}_L T_{1,j-1,k} \\ & + \bar{G}_R T_{1,j+1,k} + \bar{G}_U T_{1,j,k+1} \\ & + \bar{G}_D T_{1,j,k-1})^{n+1} + \frac{\bar{C}}{\Delta t} T^{n}_{1,j,k} \end{aligned} \tag{16}$$

where

$$j = 1 \text{ to } N_j \text{ and } k = 2 \text{ to } N_k - 1.$$

The outer convective surface can be treated in a similar way:

$$\frac{\bar{C}}{\Delta t}(T^{n+1}_{N_{i,j,k}} - T^{n}_{N_{i,j,k}}) = [\bar{G}_F(T_\infty - T_{N_{i,j,k}}) + \bar{G}_B(T_{N_{i-1,j,k}} - T_{N_{i,j,k}}) + \bar{G}_L(T_{N_{i,j-1,k}} - T_{N_{i,j,k}}) + \bar{G}_R(T_{N_{i,j+1,k}} - T_{N_{i,j,k}}) + \bar{G}_U(T_{N_{i,j,k+1}} - T_{N_{i,j,k}}) + \bar{G}_D(T_{N_{i,j,k-1}} - T_{N_{i,j,k}})]^{n+1} \quad (17)$$

where

$$\bar{G}_F = h_o R_o \Delta\theta \Delta z,$$

$$\bar{G}_B = (R_o - \Delta r/2) k_{N_{i-1/2,j,k}} \Delta\theta \Delta z/\Delta r,$$

$$\bar{G}_L = k_{N_{i,j-1/2,k}} \Delta r \Delta z/(2R_o \Delta\theta),$$

$$\bar{G}_R = k_{N_{i,j+1/2,k}} \Delta r \Delta z/(2R_o \Delta\theta),$$

$$\bar{G}_U = k_{N_{i,j,k+1/2}} (R_o - \Delta r/4)\Delta r/(2\Delta z),$$

$$\bar{G}_D = k_{N_{i,j,k-1/2}} (R_o - \Delta r/4)\Delta r/(2\Delta z),$$

$$\bar{C} = \rho c (R_o - \Delta r/4)\Delta r \Delta\theta \Delta z/2.$$

The present multi-dimensional thermal models make use of all 360° of the tube circumference. No circumferential symmetry is assumed. The computer code was written based on the above derived difference equations, and was checked against the 2-dim. (r-θ) instantaneous 4-rivulet model with 21% wetness reported in [4]. In the checkout run, 60 evenly divided circumferential nodes and 5 radial nodes were used, and the model boundary conditions were the same as in [4]. The results were in close agreement with those of [4], reflecting a temperature fluctuation between 404.4°C (760°F) and 389.4°C (733°F).

Heat transfer coefficients

Since the most severe temperature oscillations occur at the inner surface of the evaporator tube the magnitudes of the nucleate and film boiling coefficients have significant effects on the magnitudes of thermally induced stresses in the tube wall. In all previous investigations [1–4] rather high nucleate boiling coefficient based on the Jens–Lottes [9] or Thom's correlation [10] has been used. It is noted that these are essentially subcooled or very low steam quality boiling correlations, and therefore may not be suitable for the intermediate-to-high steam quality region near the CHF point under consideration. The authors feel the heat transfer mechanism prior to the occurrence of the CHF inside the evaporator tubes for the ranges of power plant steam generator thermal hydraulic conditions is that of forced convection vaporization process, for which the Chen's correlation may be more appropriate [11], Chen's pre-CHF heat transfer coefficient consists of two parts: microscopic boiling contribution and macroscopic forced convection contribution. The varying degrees of these two coefficients are added with empirically determined constants which are also a function of the Reynolds number and the Lockhart–Martinelli two-phase flow parameter. When applied to the thermal hydraulic conditions of Test No. R-78, the Chen's correlation gives a heat transfer coefficient of approximately 80 Kw/m²-°C (14,000 Btu/h-ft²-°F) which corresponds closely to the upper limit value obtained by the 1-dim. inverse heat conduction model of [12]. This value is two to three times less than the value obtainable from the Jens–Lottes correlation. The use of higher coefficients will result in unnecessarily conservative thermal stress levels on the inner surface of the heat transfer tube, and therefore Chen's correlation is adopted in the present analysis.

The film boiling heat transfer coefficient is calculated from the Bishop–Sandberg–Tong correlation [13] and 80% of this value (4.77 Kw/m²-°K) is used in the present analysis as was done in [4]. According to the concept of the revolving rivulet model, the water/steam-side heat transfer coefficient in the transition boiling region takes a distribution form of Fig. 6.

As for the outer surface sodium heat transfer coefficient, a value of 28.7 Kw/m²-°K as reported in [1] is used.

RESULTS AND DISCUSSION

Three-dimensional analysis results

In the 3-dim. revolving rivulet model, the wetness of each of these revolving rivulets is assumed to vary linearly from 100 to 0% (dryout) in the transition zone. The transition boiling zone is estimated to have a length of 38 mm (1.5 in) according to the test data from ANL-SGTF [1] and GE DNB Effects Tests [14]. The rivulet is revolving continuously from one rivulet position to another in 3 s. The 3 s period is based on the indications of test data at ANL-SGTF [1]. The 3-dim. model consists of 60 evenly divided circumferential nodes, 5 radial nodes and 26 axial nodes, thus giving a total of 7800 nodes. Fifteen of the axial nodes are located in the 38 mm (1.5 in) transition zone.

The model was run for the SGTF R-78 conditions of Table 1, and the results for three and four revolving rivulets are shown in Figs. 7 and 8, respectively. The

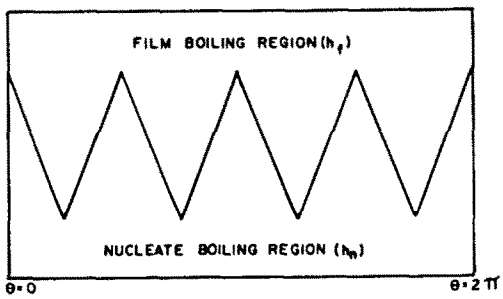

FIG. 6. Boiling heat transfer coefficient distribution for four rivulet model.

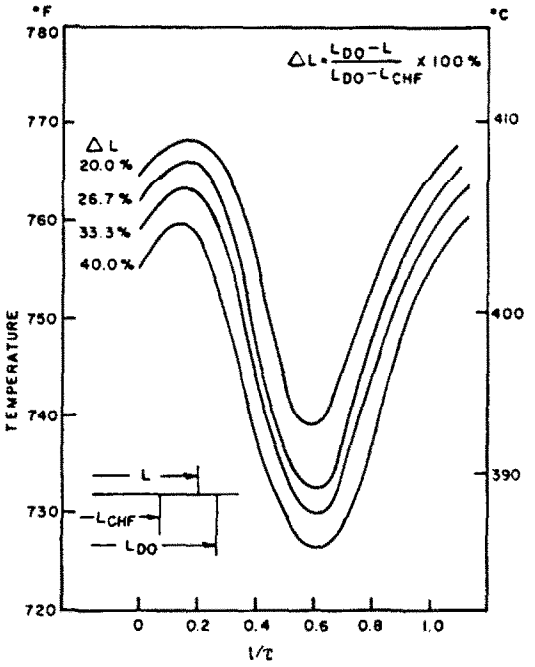

FIG. 7. Temperatures at thermocouple location for 3-dim., three rivulet model.

temperature responses at the radial depth equivalent to the thermocouple location are shown in these figures for several axial locations within the transition boiling zone (note that each axial location linearly corresponds to a different degree of circumferential wetness). As indicated in Fig. 8, the maximum temperature fluctuation is about 13.3 C (24 F) in the range of $\Delta L = 26.7$–33.3% for the four revolving

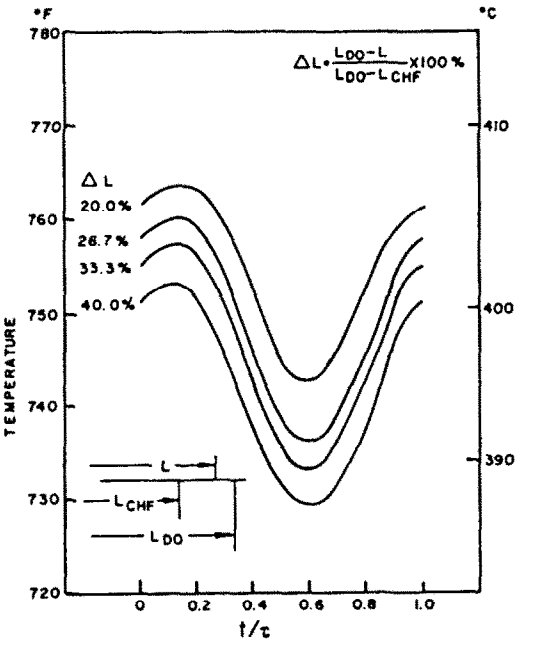

FIG. 8. Temperatures at thermocouple location for 3-dim., four rivulet model.

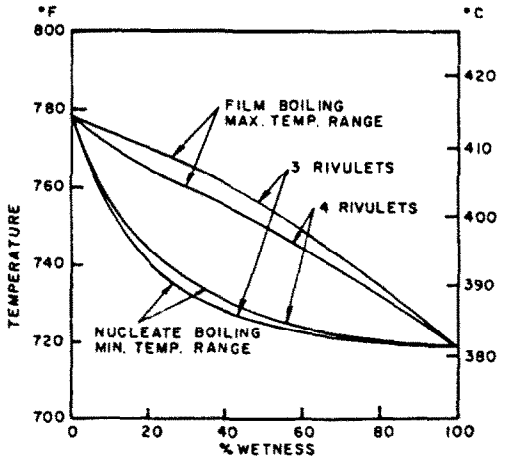

FIG. 9. Temperatures at thermocouple locations for 2-dim. (r–θ) model.

rivulet case. This compares quite favorably with the average temperature amplitude of 12.8 C (23 F) measured in the ANL-SGTF R-78.

An examination of the results for the three revolving rivulet case shown in Fig. 7 leads to a temperature fluctuation of about 18.3 C (33 F) at the 26.7–33.3% length in wetness location and this temperature fluctuation value corresponds to the maximum measured temperature oscillation range (Fig. 2). These 3-dim. results imply that the temperature oscillations in the transition zone can be represented by the formation of three or four revolving rivulets at random. The experimentally measured temperature fluctuations fall within the temperature range computed by the present model at the radial thermocouple location with the circumferential wetness between 26.7 and 33.3%. It may be noted that the runs with different axial lengths ($l > 66$ mm) result in insignificant effects on the temperature distribution in the transition boiling region.

Two-dimensional analysis results

A continuous revolving 2-dim. (r–θ) rivulet model is analyzed. All the physical properties and assumptions used are the same as those for the 3-dim. analysis. Additionally, the 2-dim. (r–θ) model requires the determination of the percentage wetness around the circumference that will match the experimental temperature fluctuations at the thermocouple location. A parametric study was made for both three and four revolving rivulet models. The maximum and minimum temperatures at the thermocouple location for both models are plotted as a function of the percentage wetness in Fig. 9. Note that the 100% wetness point corresponds to the CHF point and the 0% wetness to the complete dryout point. The experimentally measured CHF-induced temperature fluctuations for Test No. R-78 (Fig. 2) show the upper and lower bounds of the temperature fluctuations of 408 C (766 F) and 389.4 C (733 F), respectively. From Fig. 9 it can be

Table 2. Summary of multi-dimensional thermal models

Thermal models	Temperature (°C) ΔT_{T-C}	ΔT_i	ΔT_o	$\Delta(\Delta T)$
2-dim. (r, θ)				
(a) 3 rivulet, 26.7% wetness	17.5	50.1	8.2	43.1
(b) 4 rivulet, 26.7% wetness	12.2	44.2	5.3	39.5
3-dim. (r, θ, z)				
(a) 3 rivulet, 26.7–33.3% wetness	17.1	49.0	7.7	42.1
(b) 4 rivulet, 26.7–33.3% wetness	12.0	43.2	5.1	38.4

seen that the maximum and minimum temperatures of 408°C (766°F) and 390.6°C (735°F) are realizable with the 26.7% wetness for three revolving rivulets. In the four revolving rivulet model, the corresponding maximum and minimum temperatures at the thermocouple location are 405°C (761°F) and 393°C (739°F) which match closely with the average temperature fluctuations measured in the SGTF. Therefore, for a 2-dim. model $(r-\theta)$, the DNB oscillations may be represented by three to four revolving rivulets with a 26.7% wetness.

A summary of the temperature fluctuations for 2- and 3-dim. revolving rivulet models is shown in Table 2. ΔT_{T-C} is the temperature fluctuation at the radial thermocouple location; ΔT_o the maximum outer tube surface temperature fluctuation; ΔT_i the maximum inner tube wall temperature fluctuation and $\Delta(\Delta T)$ the maximum temperature oscillation between the inner and outer surfaces. Note that $\Delta(\Delta T)$ is slightly different from the difference between ΔT_i and ΔT_o. This is because the tube thermal capacity introduces a time delay effect on the temperature oscillation. It is interesting to note that the 2- and 3-dim. models give about the same temperature differences. The difference between the temperature fluctuations as obtained by the 2- and 3-dim. models is of the order of 1°C. This implies that the effect of the axial heat conduction is rather small, and can probably be neglected. A 2-dim. $(r-\theta)$ model should be quite adequate as far as thermal modeling is concerned. The computing cost of a 2-dim. model is about one order of magnitude lower than the corresponding 3-dim. model.

It should be noted that peak thermal stresses will result at the inner surface of the tube where the temperature oscillations are greatest. In this paper the temperature measurements at the thermocouple location are utilized to obtain proper modeling criteria for the design purposes.

CONCLUSIONS

Thermal analysis is performed to provide temperature distribution in the steam generator tube wall in the vicinity of the CHF point. One-, two- and three-dimensional thermal models are constructed. The region encompassing transition boiling is divided into a number of thermal nodes. Transient energy conservation equations are written for all nodes, and the resulting simultaneous equations, with appropriate boundary conditions, are solved numerically using a semi-implicit finite difference method. The oscillatory nature of the water/steam side boundary conditions in the transition boiling region is simulated by postulating a number of rivulet-type wet regions that are swirled around the tube circumference. The rate at which the rivulets are swirled or rotated is determined by the indications of ANL-SGTF DNB tests. The ANL-SGTF tests were conducted with a thermocouple imbedded inside the tube wall and the temperature history of this thermocouple has guided thermal analysis evaluations.

In a 1-dim. analysis model which is basically an inverse heat conduction problem, the thermocouple temperature vs time history is imposed on the model and the water/steam-side wall temperature predication is made as shown in Fig. 4. These results compare well with analytical solutions obtained by France *et al.*

In multi-dimensional models, three or four revolving rivulets with a 3 s period are imposed on the water/steam side of the models. The results are compared with the thermocouple temperature history. Specifically, in the 3-dim. (r, θ, z) model, the four rivulets predict favorably the average measured temperature amplitudes while the three rivulets predict the maximum temperature oscillation range, both at the axial location of 26.7 33.3% of the transition region as measured from the dryout location. Results similar to those obtained with the 3-dim. model are found with the 2-dim. (r, θ) model at the axial location corresponding to 26.7% wetness. In view of the same observations, it is concluded that the 2-dim. (r, θ) model is appropriate as far as thermal modeling of the CHF-dryout region is concerned.

Acknowledgement—This paper is based on work which was supported by the U.S. Department of Energy through Argonne National Laboratory under FWEC Contract No. 8-33-3087.

REFERENCES

1. D. M. France, T. Chiang and R. D. Carlson, Large amplitude thermal oscillations measured in an LMFBR steam generator tube, *Am. Nuc. Soc. Trans., 1977 Winter Meeting*, p. 734 (1977).
2. T. Chiang, D. M. France and T. R. Bump, Calculation of tube degradation induced by dryout instability in sodium-heated steam generators, *Nuc. Engng Des.* **41**, 181 (1977).
3. C. L. Chu, S. Wolf and A. W. Dalcher, Oscillatory dryout related thermal stresses in clean steam generator tubes, ASME Paper No. 76-JPGC-NE-2 (1976).
4. C. L. Chu, J. M. Roberts and A. W. Dalcher, DNB oscillatory temperature and thermal stress responses for evaporator tube based on rivulet model, ASME Paper No. 77-WA/NE-5 (1977).
5. F. E. Tippets, Critical heat flux and flow patterns in high pressure boiling water flows, ASME Paper No. 62-WA-162 (1962).

6. F. E. Tippets, Critical heat flux and flow pattern characteristics of high pressure boiling water in forced convection. Ph.D. thesis, Stanford University (1962).
7. N. D'Sonza, Numerical solution of one-dimensional inverse heat conduction by finite difference method, ASME Paper No. 76 WA HT-81 (1976).
8. R. D. Richtmyer and K. W. Morton, *Difference Methods for Initial Value Problems*. J. Wiley, New York (1967).
9. W. H. Jens and P. A. Lottes, Analysis of heat transfer, burnout, pressure drop, and density data for high pressure water, Argonne National Laboratory Report No. ANL-4627 (1951).
10. J. R. S. Thom, W. M. Walker, T. A. Fallon and G. F. S. Reising, Boiling in subcooled water during flow up heated tubes or annuli, Symp. on Boiling Heat Transfer in Steam Generating Units and Heat Exchangers, Inst. Mech. Engrs (1965).
11. J. C. Chen. A correlation for boiling heat transfer to saturated fluids in convective flow, ASME Paper No. 63-HT-34 (1963).
12. D. M. France and T. Chiang, Private communications on early SGTF test results for CRBR 100% and 64% load (1976).
13. A. A. Bishop, R. O. Sandberg and L. S. Tong, Forced convection heat transfer at high pressure after the critical heat flux, ASME Paper No. 65-HT-31 (1965).
14. S. Wolf and D. H. Holmes, Critical heat flux and transition boiling characteristics for a sodium-heated steam generator tube of LMFBR applications, G. E. C. Report No. FBRD-00020 (1977).

MODELE THERMIQUE DE GENERATEUR DE VAPEUR TUBULAIRE EN CHF. OSCILLATIONS DE TEMPERATURE INDUITES

Résumé—On présente des modèles analytiques pour la détermination du champ thermique dans les conditions de flux critique (CHF). Oscillations thermiques induites dans un générateur de vapeur chauffé au sodium. La nature oscillatoire des conditions aux limites convectives eau/vapeur dans l'ébullition transitoire post-CHF est simulée en postulant un nombre de régions humides semblables à des ruisselets qui sont déroulés sur la circonférence du tube. La vitesse avec laquelle les ruisselets sont déroulés ou mis en rotation est déterminée par les indications d'essais récents au Laboratoire National Argonne. Les mêmes données d'essai ont été utilisées comme critères pour le développement du modèle. Les résultats de modèles à un-deux et trois dimensions indiquent que le modèle bidimensionnel (radial-circonférentiel) avec trois ou quatre ruisselets et 26,7% de mouillage de la circonférence totale peut être convenable pour l'analyse thermique de l'ébullition de transition oscillatoire.

THERMISCHES MODELL FÜR DAMPFERZEUGER-ROHRE BEI CHF-BEDINGTEN TEMPERATUR-OSZILLATIONEN

Zusammenfassung—Zur Bestimmung des thermischen Feldes in der Wärmeübertragungsberohrung eines natriumbeheizten Dampferzeugers bei durch kritische Wärmestromdichten (CHF) bedingten thermischen Oszillationen werden analytische Modelle vorgelegt. Die oszillatorische Natur der konvektiven Randbedingungen für Wasser bzw. Dampf im Gebiet der Übergangssiedens wird durch Annahme einer Anzahl von Flüssigkeits-Strähnen simuliert, die drallartig über den Umfang laufen. Die Umlaufgeschwindigkeit der Strähnen wird unter Benutzung neuerer Meßwerte vom Argonne National Laboratory bestimmt. Die gleichen Meßwerte werden auch als Kriterium bei der Modell-Entwicklung benutzt. Die Ergebnisse der ein-, zwei- und dreidimensionalen Modelle zeigen, daß das zweidimensionale (Radial-Umfangs-) Modell mit drei oder vier Strähnen und 26,7% benetztem Umfang zur thermischen Analyse der Rohre im Bereich des oszillatorischen Übergangssiedens als geeignet angesehen werden kann.

ТЕПЛОВОЕ МОДЕЛИРОВАНИЕ СИСТЕМЫ ТРУБ ПАРОГЕНЕРАТОРА ПРИ ТЕМПЕРАТУРНЫХ КОЛЕБАНИЯХ, ВЫЗВАННЫХ КРИТИЧЕСКИМ ТЕПЛОВЫМ ПОТОКОМ

Аннотация — Представлены аналитические модели для определения теплового поля в системе теплообменных труб натриевого парогенератора при температурных колебаниях, вызванных критическим тепловым потоком. Колебательная природа конвективных условий на границе раздела водной и паровой фаз при закризисном переходном режиме кипения моделируется в предположении, что по окружности трубы имеется ряд зон смачивания вихревого типа. Скорость, с которой закручиваются или вращаются эти вихри, определяется на основе последних экспериментальных данных, полученных в Аргонской национальной лаборатории. Эти же экспериментальные данные используются в качестве критериев определения применимости предлагаемых моделей. Результаты расчетов по одно-, двух- и трехмерной моделям показывают, что двухмерная (радиально-кольцевая) модель с тремя или четырьмя вихрями и суммарной площадью смачиваемой по окружности поверхности, равной 26,7%, может успешно использоваться для теплового анализа системы теплообменных труб при колебательном переходном кипении.